J. Membrane Biol. 182, 171–181 (2001)
DOI: 10.1007/s00232-001-0042-0

The Journal of
Membrane
Biology



# Muscarinic Receptors Control $K^+$ Secretion in Inner Ear Strial Marginal Cells

**P. Wangemann,[1] J. Liu,[1] E.Q. Scherer,[1] M. Herzog,[1] M. Shimozono,[2] M.A. Scofield[3]**
[1]Cell Physiology Laboratory, Anatomy & Physiology Department Kansas State University, 1600 Dension Ave., Manhattan KS 66506, USA
[2]Otorhinolaryngology Department, Miyazaki Medical College, Miyazaki, Japan
[3]Molecular Pharmacology Laboratory, Pharmacology Department, Creighton University, Omaha NE, USA

Received: 13 November 2000/Revised: 20 April 2001

**Abstract.** $K^+$ secretion in strial marginal cells (SMC) of stria vascularis (SV) is stimulated by $\beta_1$-adrenergic receptors. The aim of the present study was to determine, whether SMC from the gerbil inner ear contain muscarinic receptors that inhibit $K^+$ secretion. Receptors were identified with pharmacological tools in functional studies where $K^+$ secretion was monitored as transepithelial current ($I_{sc}$). The cytosolic $Ca^{2+}$ concentration ($[Ca^{2+}]_i$) was measured as fluo-4 fluorescence and cAMP production with a colorimetric immunoassay. Further, receptors were identified in SV as transcripts by cloning and sequencing of reverse-transcriptase polymerase chain reaction (RT-PCR) products. The cholinergic receptor agonist carbachol (CCh) caused a transient increase in $[Ca^{2+}]_i$ with a half-maximal concentration value ($EC_{50}$) of $(5 \pm 6) \times 10^{-6}$ M ($n = 29$) and a decrease in basal and stimulated cAMP production. Apical CCh had no effect on $I_{sc}$ but basolateral CCh caused a transient increase in $I_{sc}$ with an $EC_{50}$ of $(3 \pm 1) \times 10^{-6}$ M and a sustained decrease of $I_{sc}$ with an $EC_{50}$ of $(1.2 \pm 0.2) \times 10^{-5}$ M ($n = 129$). The effects of CCh on $I_{sc}$ and $[Ca^{2+}]_i$ were inhibited in the presence of muscarinic antagonist $10^{-6}$ M atropine. Further, the muscarinic antagonists pirenzipine, methoctramine and para-fluoro-hexahydro-sila-defenidol (pFHHSiD) inhibited the CCh-induced transient increase of $I_{sc}$ with affinity constants ($K_{DB}$) of $3 \times 10^{-8}$ M ($pK_{DB} = 7.54 \pm 0.19$, $n = 17$), $2 \times 10^{-6}$ M ($pK_{DB} = 5.71 \pm 0.26$, $n = 19$) and $2 \times 10^{-8}$ M ($pK_{DB} = 7.65 \pm 0.28$, $n = 19$) and the sustained decrease of $I_{sc}$ with $K_{DB}$ of $7 \times 10^{-8}$ M ($pK_{DB} = 7.05 \pm 0.09$, $n = 33$), $6 \times 10^{-6}$ M ($pK_{DB} = 5.21 \pm 0.13$, $n = 23$), $5 \times 10^{-8}$ M ($pK_{DB} = 7.34 \pm 0.13$, $n = 31$), respectively. RT-PCR of total RNA isolated from SV using primers specific for the M1–M5 muscarinic receptors revealed products of the predicted sizes for the M3- and M4- but not the M1-, M2- and M5-muscarinic receptor subtypes. Sequence analysis confirmed that amplified cDNA fragments encoded gene-specific nucleotide sequences. These results suggest that $K^+$ secretion in SMC is under the control of M3- and M4-muscarinic receptors that may be located in the basolateral membrane of strial marginal cells.

**Key words:** Stria vascularis — Cochlea — Pirenzipine — Methoctramine — pFHHSiD

## Introduction

Scala media, the fluid compartment adjacent to the sensory hair cells in the cochlea, is filled with endolymph, which is an unusual extracellular fluid in that it contains 150 mM $K^+$ and no more than 1 mM $Na^+$. The $K^+$ content of scala media provides a reservoir of charge carrier for the sensory transduction process and determines the volume and the mechanical properties of this mechanosensitive organ. $K^+$ is secreted into cochlear endolymph by strial marginal cells (SMC) of the stria vascularis. The rate of $K^+$ secretion by SMC is one of the main factors that contribute to the homeostasis of endolymph, although cochlear endolymph is enclosed by about twelve different epithelial cell types, each of which may contribute to the homeostasis of this extracellular fluid space (Wangemann, 1995).

Recently it was shown that the rate of $K^+$ secretion by SMC is stimulated by a number of factors such as an elevated basolateral $K^+$ concentration, an acidic pH or an increased cell volume (Wangemann, Liu & Marcus, 1995; Wangemann, Liu & Shiga, 1996; P. Wangemann, *unpublished observations*). Further, it was shown that $K^+$ secretion in SMC is stimulated via $\beta_1$-adrenergic recep-

*Correspondence to:* P. Wangemann

tors, which signal via $G_s$ protein and cause a stimulation of adenylyl cyclase and an increase in the cAMP production (Wangemann et al., 2000). In general, sympathetic stimulation mediated via β-adrenergic receptors is often balanced by parasympathetic inhibition mediated via acetylcholine receptors. Based on the understanding that stria vascularis does not contain nicotinic acetylcholine receptors (Morley et al., 1998), we hypothesized that SMC contain muscarinic receptors that cause an inhibition of $K^+$ secretion.

In general, of the five known muscarinic receptor subtypes (M1–M5), the even numbered receptors M2 and M4 signal an inhibition of adenylyl cyclase, mainly via $G_i$, and the odd-numbered receptors signal an increase in the cytosolic $Ca^{2+}$ concentration, mainly via $G_q$ (Alexander, Peters & Mead, 1998). Pharmacological tools are now well established to identify muscarinic acetylcholine receptors in the absence of nicotinic acetylcholine receptors. Muscarinic acetylcholine receptors can be identified by the nonspecific agonist CCh, which mimics the effects of the natural agonists acetylcholine, in conjunction with antagonists such as atropine, which prevent agonist-induced effects. Further, the muscarinic acetylcholine receptor subtypes M1, M2 and M3 can be distinguished pharmacologically by the affinities of the antagonists pirenzipine, methoctramine and para-fluorohexahydo-sila-defenidol (pFHHSiD). Pharmacological tools to distinguish between the M4 and M5 muscarinic acetylcholine receptor subtypes, however, are not yet well established (Caulfield & Birdsall, 1998). In addition, evidence for the presence of muscarinic acetylcholine receptor subtypes can be obtained with molecular techniques. Parts of the present study have been presented at recent meetings (Liu & Wangemann, 1998; Shimozono, Scofield & Wangemann, 1998).

## Materials and Methods

### Preparations

The method of isolation of stria vascularis has been described previously (Wangemann et al., 1995). Briefly, gerbils were deeply anesthetized with pentobarbital (100 mg/kg i.p.) and decapitated. The procedures concerning animals reported in this study were approved by the Institutional Animal Care and Use Committee at Boys Town National Research Hospital and Kansas State University. The temporal bones containing the inner ear were removed and quickly transferred for microdissection into cold (4°C) $Cl^-$-free solution, which contained (in mM) 150 Na-gluconate, 1.6 $K_2HPO_4$, 0.4 $KH_2PO_4$, 4.0 Ca-gluconate, 1.0 $MgSO_4$, 5.0 glucose pH 7.4. Stria vascularis was removed from spiral ligament under microscopic observation. For an illustration of the dissection, *see* Wangemann et al. (2000). For the measurement of $I_{sc}$, stria vascularis from the second turn was used as a flat sheet. For the measurements of $[Ca^{2+}]_i$, stria vascularis was folded into a loop. For molecular biological and biochemical studies, stria vascularis was collected from all turns of the cochlea. Further, brain and blood were collected for control experiments in the molecular biological studies.

### Measurements of Equivalent Short Circuit Current

The equivalent short circuit current ($I_{sc}$), which can be obtained from measurements of the transepithelial voltage and transepithelial resistance, has been shown to be a measure for the rate of transepithelial $K^+$ secretion (Wangemann et al., 1995). SMC generate an apical-side positive transepithelial voltage when both sides of the epithelium are bathed with a symmetrical NaCl solution (Wangemann et al., 1995). This solution contained (in mM) 150 NaCl, 1.6 $K_2HPO_4$, 0.4 $KH_2PO_4$, 0.7 $CaCl_2$, 1.0 $MgSO_4$, and 5.0 glucose, pH 7.4. The transepithelial voltage, which is generated under these conditions, is due to the electromotive forces associated with the $K^+$-conductive apical membrane and the $Cl^-$-conductive basolateral membrane. Methods for the measurement of the transepithelial voltage and transepithelial resistance were described previously (Wangemann et al., 1995). Briefly, stria vascularis was mounted in a micro-Ussing chamber by sealing the apical membrane of SMC to the aperture (80 μm diameter). In this configuration, SMC were virtually isolated. The transepithelial voltage and resistance are generated solely across the SMC barrier (Wangemann et al., 1995). Consequently, effects on the equivalent short circuit current were attributed to SMC. Although other cells of stria vascularis were present, they were short-circuited and did not contribute to the transepithelial voltage measured in this preparation. This is in particular important with regard to basal cells, which form a barrier in vivo. The basal cell barrier, however, does not persist in vitro due to unavoidable damage in the separation of stria vascularis from the spiral ligament. The apical and basolateral sides SMC were perfused separately and exchange of solution on each side was complete within 1 sec. Transepithelial voltage ($V_t$) was measured with calomel electrodes connected to the chambers via 1 M KCl bridges. The transepithelial resistance ($R_t$) was obtained from the voltage changes induced by current pulses (50 nA for 34 msec at 0.3 Hz). Sample and hold circuitry was used to obtain a signal proportional to $R_t$. The equivalent short circuit current ($I_{sc}$) was obtained according to Ohm's law ($I_{sc} = V_t/R_t$) from measurements of $V_t$ and $R_t$.

### Measurements of the Cytosolic $Ca^{2+}$ Concentration

Stria vascularis was incubated for 20 min with 5 μM fluo-4-AM at 37°C to load the cells with the $Ca^{2+}$-indicator dye fluo-4 (Molecular Probes, Eugene, OR). Subsequently the tissue was folded into a loop and mounted in the superfusion chamber on the stage of an inverted microscope (Diaphot, Nikon). The preparation was alternately illuminated with light of 600 and 488 nm (Deltascan, Photon Technology International, South Brunswick, N.J.). Epilumination was chosen for the 488 nm light path and transillumination for the 600 nm light path. The 488 nm light was reflected on a 515 nm dichroic mirror (Omega Optical, Brattleboro, VT) to reach the preparation. The fluorescence (500–550 nm) emitted in response to 488 nm excitation was transmitted through the 515 nm dichroic mirror, reflected by a 580 nm dichroic mirror (Nikon) and limited with a band-pass filter to a wavelength between 518 and 542 nm (Omega Optical). The fluorescence signal was then recorded by a photon-counter (Photon Technology International) at a rate of 4 Hz. Changes in the emission intensity were taken as measures of changes in $[Ca^{2+}]_i$. The image observed with the 600 nm light was transmitted through the 515 and 580 nm dichroic mirrors, detected by a chilled CCD camera (C5985-02, Hamamatsu) at a rate of 0.25 Hz and displayed on a monitor (PVM-137, Sony) for observation. For a schematic diagram of the setup for simultaneous fluorescence and videomicroscopy measurements, *see* Scherer et al. (2001).

## Measurements of cAMP Production

Stria vascularis was obtained by microdissection in $Cl^-$ free solution (*see above*) and used within one hour after sacrifice of the animal. Tissues were pooled from two ears and divided into four apparently equal samples. Methods for measuring cAMP-production were modified from an original protocol described elsewhere (Wangemann et al., 2000). Briefly, tissue samples were transferred into a NaCl solution (*see above*), which contained the phosphodiesterase inhibitor (2 mM) 3-isobutyl-1-methylxanthine (Sigma). After 6 min equilibration with agitation at 37°C, an aliquot of NaCl solution either without agonists, with CCh, with isoproterenol or with CCh and isoproterenol was added. Samples (46 μl) were then incubated with agitation for 12 min at 37°C. Incubation at 37°C with agitation may be important since β-adrenergic receptor signaling appears to be sensitive to temperature and metabolic compromise (Wangemann et al., 2000). After the incubation, the reaction was stopped by addition of the lysis reagent containing dodecyltrimethylammonium bromide. Tissues were disrupted by sonication and undissolved tissue fragments were removed by centrifugation. cAMP in the supernatant was then measured with a colorimetric immunoassay according to the protocol specified by the manufacturers (RPN 225 Amersham, Piscataway, NJ).

## Data Analysis

Dose-response curves were obtained by testing in one tissue sample the effect of only one concentration of agonist in the absence and presence of one concentration of antagonist as shown in Fig. 2. It was not possible to obtain cumulative dose-response curves since preliminary experiments revealed that the effect of additional doses was significantly smaller compared to experiments in which only two doses had been given.

The agonist concentration, which induced a half-maximal effect ($EC_{50}$), was obtained by fitting data to the equation

$$E = 100 \times C^h/(EC_{50}{}^h + C^h) \quad (1)$$

where $E$ is the change in $I_{sc}$ or fluorescence relative to the maximal CCh-induced change, $C$ is the concentration of agonist and $h$ is the slope. In detail, $1 \times 10^{-3}$ M CCh caused a transient increase in $I_{sc}$ from $921 \pm 66$ to $1078 \pm 81$ μA/cm$^2$ ($n = 7$) corresponding to $17 \pm 3\%$. This transient increase was followed by a sustained decrease in $I_{sc}$ to $194 \pm 41$ μA/cm$^2$ ($n = 7$) corresponding to an inhibition of $79 \pm 9\%$. The affinity of antagonists to the receptor ($K_{DB}$) was obtained through competitive inhibition using CCh as the agonist. $K_{DB}$ was obtained from the Schild-equation

$$p(K_{DB}) = \log(B) - \log(DR\text{-}1) \quad (2)$$

where $B$ is the concentration of the antagonist and $DR$ is the dose-ratio. DR was obtained according to

$$DR = EC_{50\ Antagonist}/EC_{50CCh} \quad (3)$$

where $EC_{50\ Antagonist}$ is the $EC_{50}$ of CCh in the presence of the antagonist and $EC_{50CCh}$ is the $EC_{50}$ of CCh in the absence of antagonist. $EC_{50\ Antagonist}$ was obtained according to equation (*1*) in which $E_{max}$ and $h$ were fixed to the values obtained in the absence of antagonists. All nonlinear curve fits were obtained by a least-squares algorithm using a programmable spreadsheet and plotting software (Origin 4.1 or 6.0, Microcal, Northampton, MA).

## Demonstration of Receptor-specific Transcripts

### *Extraction of Total RNA*

Total RNA was extracted from blood, brain and stria vascularis as described earlier (Wangemann et al., 1999). Briefly, methods employed for the extraction of RNA from stria vascularis were different from those employed for blood and brain due to the lower amount of RNA available in stria vascularis. Fresh blood was transferred into TRIzol Reagent (GIBCO BRL, Life Technologies) and total RNA was extracted according to manufacturer's procedure. Brains were frozen in liquid nitrogen within 5 min of sacrifice. The frozen tissue was pulverized in liquid nitrogen and immediately transferred into TRIzol Reagent (GIBCO BRL, Life Technologies). Total RNA was extracted using the TRIzol Reagent according to manufacturer's procedure. The nucleic acid concentrations were determined spectrophotometrically and adjusted to be between 1.0 and 2.0 μg/μl. RNA samples were stored at −70°C. Before analysis of the RNA samples by reverse-transcription polymerase chain reaction (RT-PCR), DNA contamination of the RNA samples was removed by treatment with DNase I (GIBCO BRL, Life Technologies) in the presence of RNasin (Promega) for 30 minutes at 37°C. DNAse I was removed by phenol-chloroform extraction and precipitation of total RNA with ethanol in the presence of 2 M $NH_4OAC$.

Stria vascularis was isolated by microdissection in $Cl^-$-free solution (*see above*) and directly transferred from the dissection medium into the TRIzol Reagent within 7 min (first ear) and 15 min (second ear) of sacrifice of each animal. Tissues from eight ears were pooled in the TRIzol Reagent and disrupted by sheer stress induced by a 25 gauge hypodermic syringe needle. Total RNA from stria vascularis was extracted using the TRIzol Reagent according to the manufacturer's procedure. The final nucleotide concentration of the RNA samples from stria vascularis was adjusted to 0.3 μg/μl. RNA samples were stored at −70°C. Residual genomic DNA in RNA samples from stria vascularis was removed prior to RT-PCR by treatment with amplification-grade RNase-free DNase I (GIBCO BRL, Life Technologies) for 30 minutes at room temperature followed by heat inactivation in the presence of EDTA, according to the protocol specified by the manufacturers.

### *cDNA Synthesis and PCR Amplification*

Total RNA was reverse transcribed into cDNA in a 20 μl reaction. The reaction contained 0.20–0.30 μg total RNA, 20 units RNasin (Promega), 1 mM dNTP (GIBCO BRL), 50 units Moloney Murine Leukemia Virus Reverse Transcriptase (Perkin-Elmer), 2.5 mM $MgCl_2$ (GIBCO BRL), 25 pmol oligo d(T), 20 mM Tris-HCl and 50 mM KCl. Tris-HCl and KCl were added from a 10× PCR buffer (GIBCO BRL). The RT reaction was incubated for 15 min at room temperature (25°C), then for 50 min at 42°C, for 5 min at 99°C, and finally for 5 min at 5°C.

The 100 μl PCR reaction contained the 20 μl RT reaction mix, 2.5 units Taq DNA polymerase (GIBCO BRL) and 25 pmol of the antisense and the sense primer for the M1, M2, M3, M4 or M5 muscarinic acetylcholine receptor, respectively. The primers used are shown in Table 1. The final concentrations of $MgCl_2$ , KCl and Tris-HCl were adjusted to 2.5, 50 and 20 mM, respectively. The PCR reaction mix was incubated as follows: denaturation for 3 min at 95°C; 45 amplification cycles consisting of 1 min denaturation at 95°C, 1 min annealing at 55°C and 1 min extension at 72°C; and 1 extension cycle for 5 min at 72°C. PCR products were analyzed by horizontal electrophoresis in 2% agarose gels and visualized by ethidium bromide.

### *Cloning and Sequencing of Amplified cDNA Fragments*

Amplified cDNA fragments were extracted from the agarose gels using the QIA quick gel extraction kit (Qiagen) and cloned into a pCR®2.1

**Table 1.** Primers

| Subtype | Orientation | Primer | Location* | Size |
|---|---|---|---|---|
| $m_1$ | sense | 5′-CTGGTTTCCTTCGTTCTCTG-3′ | 593–612 | 641 bp |
| | antisense | 5′-GCTGCCTTCTTCTCCTTGAC-3′ | 1214–1233 | |
| $m_2$ | sense | 5′-GGCAAGCAAGAGTAGAATAAA-3′ | 1084–1104 | 552 bp |
| | antisense | 5′-GCCAACAGGATAGCCAAGATT-3′ | 1615–1635 | |
| $m_3$ | sense | 5′-GTGGTGTGATGATTGGTCTG-3′ | 2682–2701 | 790 bp |
| | antisense | 5′-TCTGCCGAGGAGTTGGTGTC-3′ | 3452–3471 | |
| $m_4$ | sense | 5′-TGGAGACAGTGGAGATGGTG-3′ | 72–91 | 538 bp |
| | antisense | 5′-AGGTAGAAGGCAGCAATGG-3′ | 591–609 | |
| $m_5$ | sense | 5′-CTCATCATTGGCATCTTCTCCA-3′ | 1199–1220 | 451 bp |
| | antisense | 5′-GGTCCTTGGTTCGCTTCTCTGT-3′ | 1628–1649 | |

* according to known sequences in the rat (accession #): $m_1$ M16406, $m_2$ J03025, $m_3$ M62826, $m_4$ M16409 and $m_5$ M22926

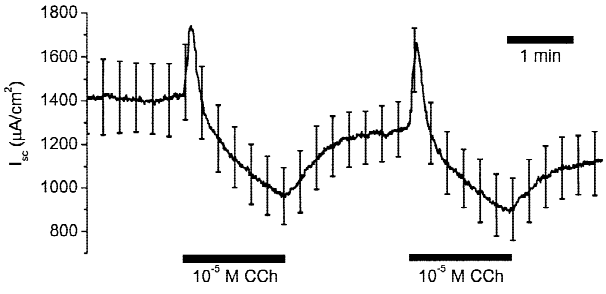


**Fig. 1.** Effect of carbachol (CCh) on $I_{sc}$. The average of 6 experiments is shown. For clarity, not all error bars are shown. Note that the biphasic effect of CCh is reversible and repeatable.

vector with a TA cloning® kit (Invitrogen). Recombinant plasmids were isolated from positive colonies using the standard alkaline lysis procedure, purified by phenol/chloroform extraction, and precipitated and washed with ethanol. Insertion of the PCR product into the plasmid was confirmed by restriction endonuclease digestion with *Eco*RI and subsequent horizontal gel electrophoresis. The recombinant double stranded plasmid served as a template for cycle sequencing using M13 forward and reverse primers and fluorescence-based dideoxy nucleotides (PRISM Ready Reaction Dye Deoxy Terminator Cycle Sequencing Kit, Perkin Elmer). The sequence was then determined using the ABI Model 373 DNA Sequencer (Applied Biosystems) and confirmed by the cloning and sequencing of RT-PCR products from at least three separate RT-PCR reactions. The identity of the gerbil sequences was determined by a FastA (Wisconsin Package, Genetics Computer Group) comparison to known GenBank/EMBL sequences.

### Statistics

Data of functional studies are presented as the mean ± SEM. The number of observations ($n$) is the number of tissues or the number of independent assays. Student's $t$-test of paired samples was applied and a level of $P < 0.05$ taken as statistically significant.

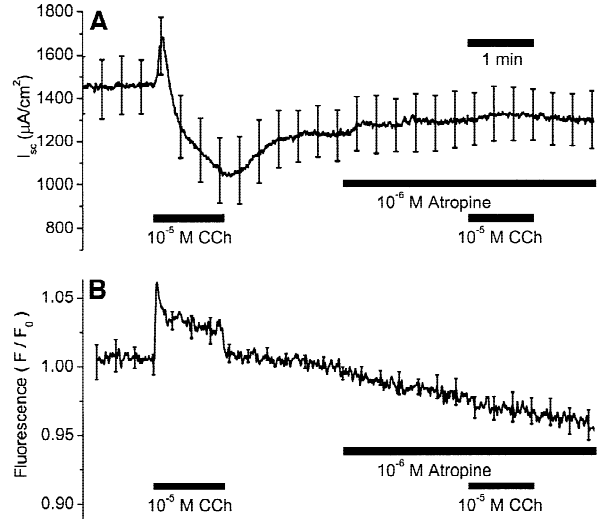


**Fig. 2.** Effect of carbachol (CCh) in the absence and presence of the muscarinic antagonist atropine. (*A*) Effect of CCh on $I_{sc}$. An average of 6 experiments is shown. (*B*) Effect of CCh on fluo-4 fluorescence (cytosolic $Ca^{2+}$ concentration). An average of 7 experiments is shown. For clarity, not all error bars are shown in *A* and *B*. Note that CCh caused a transient increase in $I_{sc}$ and fluo-4 fluorescence and that atropine prevents these effects.

## Results

### Functional Studies

A well-known agonist/antagonist pair for muscarinic acetylcholine receptors in the absence of nicotinic acetylcholine receptors are the nonspecific agonist CCh and the antagonist atropine. If muscarinic acetylcholine receptors were linked to the regulation of $K^+$ secretion in SMC, it would be expected that the agonist CCh causes a change in $I_{sc}$ and that this effect would be absent in the

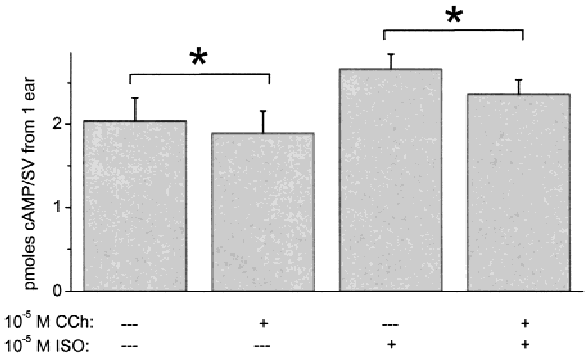


**Fig. 3.** Effect of $10^{-5}$ M carbachol (CCh) on cAMP production in the absence and presence of stimulation with the β-adrenergic receptor agonist $10^{-5}$ M isoproterenol (ISO). Averages of 7 paired experiments are shown. *Denotes a significant difference.

presence of the antagonist atropine. Thus, in a first series of experiments the effects of CCh on $I_{sc}$ were determined. CCh ($10^{-5}$ M) had no significant effect on $I_{sc}$ when added to the apical perfusate (1447 ± 156 versus 1454 ± 142 μA/cm$^2$, $n = 8$). When added to the basolateral perfusate, CCh caused a transient increase in $I_{sc}$, which was followed by a sustained decrease. These effects were reversible and repeatable (Fig. 1). The transient increase was dose-dependent with an $EC_{50}$ of (3 ± 1) × $10^{-6}$ M and $h$ of 1.7 ± 0.4 ($n = 133$) and the sustained decrease of $I_{sc}$ after 90 sec was dose-dependent with an $EC_{50}$ of (5 ± 2) × $10^{-5}$ M and $h$ of 0.74 ± 0.07 ($n = 129$). The observation that $h$ was significantly different from 1 remains unexplained. In a second series of paired experiments the effect of CCh on $I_{sc}$ in the absence and presence of atropine was determined. Atropine by itself had a small but significant effect on $I_{sc}$. Indeed, $I_{sc}$ increased by 3.5 ± 1.5% (from 1231 ± 121 to 1274 ± 130 μA/cm$^2$, $n = 6$). The transient increase and the subsequent sustained decrease induced by $10^{-5}$ M CCh were absent in the presence of $10^{-6}$ M atropine (Fig. 2*A*). These findings are consistent with the conclusion that the rate of $K^+$ secretion in SMC is controlled by muscarinic acetylcholine receptors.

If muscarinic acetylcholine receptors in stria vascu-

**Table 2.** $K_{DB}$ values for cloned muscarinic receptors

| Receptor Subtype | $K_{DB}$ Antagonist | | | Citation |
|---|---|---|---|---|
| | Pirenzipine | Methoctramine | pFHHSiD | |
| M1 | 1.22E-08 | — | 5.57E-08 | Chen et al., 1995 |
| | 1.60E-08 | 1.60E-08 | — | Buckley et al., 1989 |
| | 2.00E-08 | 5.01E-07 | 2.51E-07 | Brauner-Osborne & Brann, 1996 |
| | 1.30E-08 | — | — | Kashihara et al., 1992 |
| | 4.47E-09 | 6.92E-08 | — | Lazareno & Birdsall, 1993 |
| | 6.31E-09 | 5.01E-08 | 2.24E-08 | Dorje et al., 1991 |
| M2 | 4.43E-07 | — | 1.32E-07 | Chen et al. 1995 |
| | 9.06E-07 | 3.60E-09 | — | Buckley et al., 1989 |
| | 6.31E-07 | 2.51E-08 | 5.01E-07 | Brauner-Osborne & Brann, 1996 |
| | 4.18E-07 | 4.40E-08 | — | Kashihara et al., 1992 |
| | 2.24E-07 | 1.32E-08 | 1.32E-07 | Dorje et al., 1991 |
| | 2.24E-07 | 6.92E-09 | — | Lazareno & Birdsall, 1993 |
| M3 | 1.65E-07 | — | 1.98E-08 | Chen et al., 1995 |
| | 1.80E-07 | 1.18E-07 | — | Buckley et al., 1989 |
| | 2.51E-07 | 1.00E-06 | 3.16E-08 | Brauner-Osborne & Brann, 1996 |
| | 1.90E-07 | — | — | Kashihara et al., 1992 |
| | 1.38E-07 | 2.14E-07 | 1.55E-08 | Dorje et al., 1991 |
| | 1.32E-07 | 5.37E-07 | — | Lazareno & Birdsall, 1993 |
| M4 | 6.81E-08 | — | 3.16E-08 | Chen et al., 1995 |
| | 5.01E-08 | 3.98E-07 | 5.01E-08 | Brauner-Osborne & Brann, 1996 |
| | 8.50E-08 | — | — | Kashihara et al., 1992 |
| | 3.72E-08 | 3.16E-08 | 3.16E-08 | Dorje et al., 1991 |
| M5 | — | 5.70E-08 | — | Buckley et al., 1989 |
| | 1.26E-07 | 1.00E-06 | 7.94E-08 | Brauner-Osborne & Brann, 1996 |
| | 8.70E_08 | — | — | Kashihara et al., 1992 |
| | 8.91E-08 | 1.35E-07 | 9.33E-08 | Dorje et al., 1991 |

**Table 3.** $K_{DB}$ values for native muscarinic receptors

| Receptor | Pirenzipine | Methoctramine | pFHHSiD | Citation |
|---|---|---|---|---|
| M1 | 9.55E-09 | — | 2.09E-07 | Bognar et al., 1992 |
| | 3.72E-08 | — | — | Doods et al., 1987 |
| | 8.32E-09 | — | 1.70E-07 | Eltze, 1996 |
| | 1.26E-08 | 7.94E-08 | — | Hulme et al., 1990 |
| | 7.94E-09 | — | — | Hulme et al., 1990 |
| | 9.55E-09 | 2.51E-08 | — | Lazareno et al., 1990 |
| | 5.00E-09 | 5.00E-08 | — | Waelbroeck et al., 1990 |
| M2 | 1.07E-07 | 8.80E-08 | — | Buckley et al., 1989 |
| | 1.02E-06 | — | 9.16E-07 | Cuq et al., 1994 |
| | 6.92E-08 | — | 7.24E-09 | Dehaye et al., 1988 |
| | 1.38E-06 | — | — | Doods et al., 1987 |
| | 5.89E-07 | — | 8.13E-07 | Eltze, 1996 |
| | 5.12E-07 | 7.40E-09 | — | Goodwin et al., 1995 |
| | 5.01E-07 | 1.26E-08 | — | Hulme et al., 1990 |
| | 3.16E-07 | 1.58E-08 | — | Hulme et al., 1990 |
| | 3.31E-07 | 4.57E-09 | — | Lazareno et al., 1990 |
| | 3.50E-07 | 1.30E-08 | — | Waelbroeck et al., 1990 |
| | 2.14E-07 | — | 6.31E-07 | Bognar et al., 1992 |
| M3 | 2.19E-07 | — | 1.45E-08 | Bognar et al., 1992 |
| | 4.17E-07 | — | — | Doods et al., 1987 |
| | 1.35E-07 | — | 3.24E-08 | Eltze, 1996 |
| | 1.58E-07 | 3.16E-07 | — | Hulme et al., 1990 |
| | 1.58E-07 | 6.31E-07 | — | Hulme et al., 1990 |
| | 8.13E-08 | 1.32E-07 | — | Lazareno et al., 1990 |
| | 1.50E-07 | 1.00E-06 | — | Waelbroeck et al., 1990 |
| | 6.49E-07 | 1.00E-06 | — | Eltze, 1996 |
| M4 | 2.51E-08 | 1.38E-08 | — | Lazareno et al., 1990 |
| | 3.39E-08 | 1.55E-08 | — | Lazareno et al., 1990 |
| | 8.00E_08 | 2.30E-08 | — | Waelbroeck et al., 1990 |

laris included subtypes M1, M3 and/or M5, it would be expected that CCh causes an increase in $[Ca^{2+}]_i$ whereas such an increase would not be as likely if only the subtypes M2 and/or M4 were involved. Thus, in a third series of paired experiments, the effect of CCh on $[Ca^{2+}]_i$ was determined. CCh caused a transient increase in $[Ca^{2+}]_i$ that was dose-dependent with an $EC_{50}$ of $(5 \pm 6) \times 10^{-6}$ M and $h$ of $0.69 \pm 0.54$ ($n = 29$). Dose-response curves for the initial transient effect on $[Ca^{2+}]_i$ and $I_{sc}$ were superimposable. As expected from the observation on $I_{sc}$, the effect of $10^{-5}$ M CCh on $[Ca^{2+}]_i$ was fully inhibited in the presence of $10^{-6}$ M atropine (Fig. 2*B*). These observations suggest that stria marginal cells contain M1, M3 and/or M5 muscarinic receptors.

Alternatively, if muscarinic acetylcholine receptors in stria vascularis included subtypes M2 and/or M4, it would be expected that CCh causes a decrease in the cytosolic cAMP concentration whereas such a decrease would not be as likely if only the subtypes M1, M3 and/or M5 were involved. Thus, in a fourth series of paired experiments, the effect of CCh on cAMP production was determined. CCh caused a significant decrease in the unstimulated and isoproterenol-stimulated cAMP production (Fig. 3). These observations suggest that stria vascularis contains M2 and/or M4 receptors or that the observed inhibitory effect on adenylyl cyclase is secondary in nature.

Several studies have provided pharmacologic characterizations of muscarinic acetylcholine receptors (Table 2 and 3). A review of this literature suggests that there are three antagonists namely pirenzipine, methoctramine and pFHHSiD, which can distinguish well between the M1, M2 and M3 muscarinic acetylcholine receptor subtypes. Pharmacologic tools to unambiguously determine the presence of the M4 and M5 subtypes are apparently still lacking. Thus, the dominating receptor subtype reducing $K^+$ secretion in SMC can be determined pharmacologically as long as it is one among M1, M2 and M3. In a fifth series of paired experiments the effects of pirenzipine, methoctramine and pFHHSiD on CCh-induced stimulation of $I_{sc}$ was determined. By themselves, these antagonists caused small but significant increases in $I_{sc}$ similar to those observed in presence of atropine. In detail, $10^{-7}$ M pirenzipine had no significant effect ($n = 19$), but $10^{-6}$ M pirenzipine increased $I_{sc}$ by $5 \pm 1\%$ ($n = 12$). Methoctramine $10^{-5}$ and $10^{-4}$ M

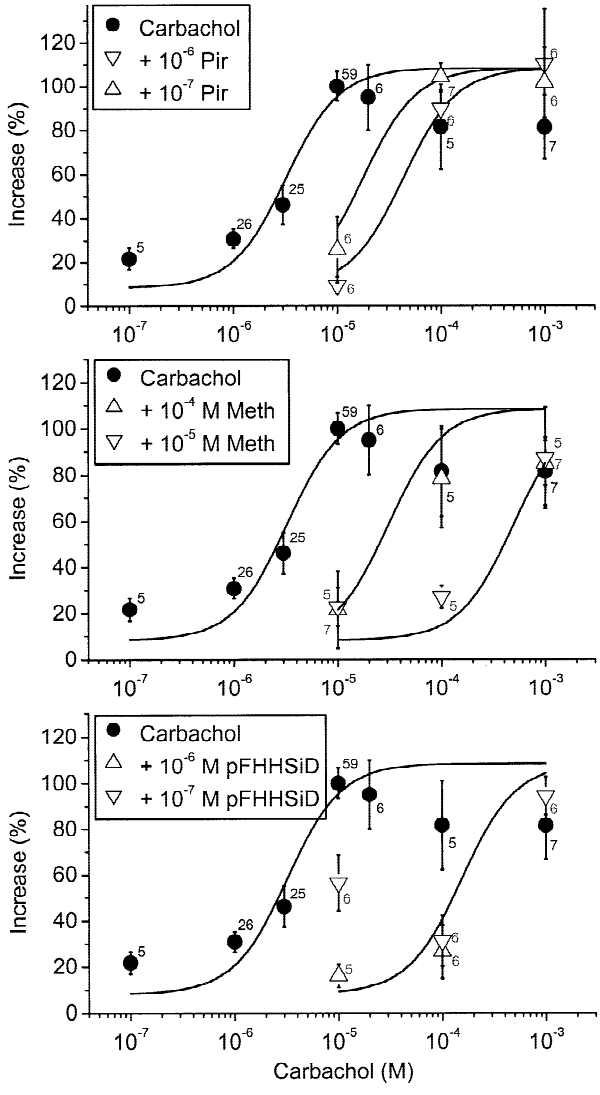


**Fig. 4.** Dose-response curves for the carbachol-induced transient increase of $I_{sc}$ in the absence and presence of the muscarinic antagonists pirenzipine (*top*), methoctramine (*middle*) and pFHHSiD (*bottom*). Data were normalized to the percentage (17%) by which $1 \times 10^{-5}$ M CCh increased $I_{sc}$ in the absence of antagonists. The dose-response curve for CCh in the absence of antagonists has been added to each graph for comparison. Curves are the result of a nonlinear fit to equation *1* (*see* Methods). The numbers next to the symbols depict the number of experiments.

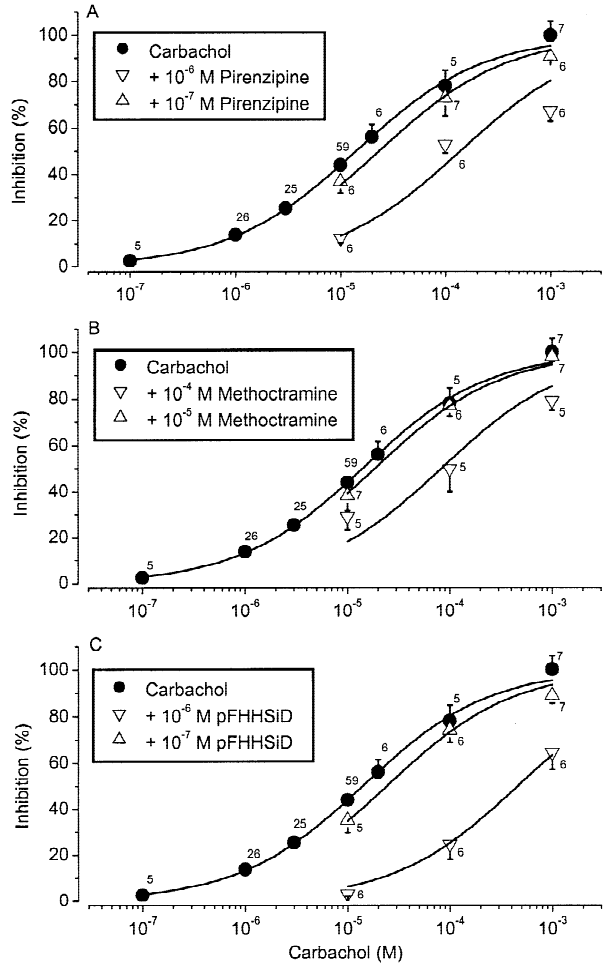


**Fig. 5.** Dose-response curves for the carbachol-induced sustained decrease of $I_{sc}$ in the absence and presence of the muscarinic antagonists pirenzipine (*top*), methoctramine (*middle*) and pFHHSiD (*bottom*). Data were normalized to the percentage (79%) by which $1 \times 10^{-3}$ M CCh reduced $I_{sc}$ in the absence of antagonists. The dose-response curve for CCh in the absence of antagonists has been added to each graph for comparison. Curves are the result of a nonlinear fit to equation *1* (*see* Methods). The numbers next to the symbols depict the number of experiments.

increased $I_{sc}$ by 3 ± 1% ($n = 20$) and 8 ± 3% ($n = 10$), respectively. pFHHSiD $10^{-7}$ M increased $I_{sc}$ by 2 ± 1% ($n = 18$) but $10^{-6}$ M pFHHSiD had no significant effect ($n = 12$). In the presence of pirenzipine, methroctramine or pFHHSiD the dose-response curves for CCh were shifted to the right as expected for competitive inhibitors. Dose-response curves are summarized in Fig. 4 and 5 and $K_{DB}$ values are given in Table 4. Comparison of these $K_{DB}$ values with $K_{DB}$ values for cloned or native receptors suggests that $K^+$ secretion in SMC is predominantly modulated via a muscarinic acetylcholine receptor that is pharmacologically most closely related to the M3 and M4 subtypes (*see* Discussion).

## Molecular Studies

In addition to the pharmacological characterization of functional muscarinic acetylcholine receptor subtypes, the presence of transcripts was determined by RT-PCR of total RNA isolated from stria vascularis. In a sixth series of experiments RT-PCR was performed on total RNA from stria vascularis, brain and blood using primers specific for the gerbil M1, M2, M3, M4 and M5 musca-

**Table 4.** $K_{DB}$ values for muscarinic antagonists

| Antagonist | Parameter | $pK_{DB}$ | $n$ | $K_{DB}$ |
|---|---|---|---|---|
| Pirenzipine | Transient stimulation | 7.54 ± 0.19 | 17 | $3 \times 10^{-8}$ |
| | Sustained inhibition | 7.15 ± 0.09 | 33 | $7 \times 10^{-8}$ |
| Methoctramine | Transient stimulation | 5.71 + 0.26 | 19 | $2 \times 10^{-6}$ |
| | Sustained inhibition | 5.21 ± 0.13 | 23 | $6 \times 10^{-6}$ |
| pFHHSiD | Transient stimulation | 7.65 + 0.28 | 19 | $2 \times 10^{-8}$ |
| | Sustained inhibition | 7.34 ± 0.13 | 31 | $5 \times 10^{-8}$ |

rinic acetylcholine receptor transcripts. Total RNA was isolated from stria vascularis rather than from SMC because RNA cannot readily be obtained from SMC. Reactions performed on total RNA from stria vascularis with primers specific for M3 and M4 muscarinic acetylcholine receptor subtypes revealed products of the expected size of 790 and 538 bp, respectively (Fig. 6, lanes marked 'SV +'). No appropriate product was found in reactions performed with primers specific for the M1, M2 and M5 muscarinic acetylcholine receptor subtypes. These observations suggest that stria vascularis contains transcripts for M3 and M4 but not for the M1, M2 and M5 muscarinic acetylcholine receptor subtypes. The specificity of the primers was verified through RT-PCR performed with total RNA extracted from gerbil brain with primers specific for the M1, M2, M3, M4 and M5 muscarinic acetylcholine receptor (Fig. 6, lanes marked 'Brain +'). These reactions revealed products of the expected size of 641 bp, 552 bp, 790 bp, 538 bp and 451 bp, respectively. The identities of all appropriate PCR products were defined by sequence analysis. Comparison of the sequences to known sequences verified that they are fragments of M1, M2, M3, M4 and M5 muscarinic acetylcholine receptor subtypes, respectively. Sequences of the amplified gerbil stria vascularis M3 and M4 muscarinic acetylcholine receptor transcripts were identical to those amplified from the gerbil brain. Sequences for the M1, M2, M3, M4 and M5 muscarinic acetylcholine receptor fragments were deposited in GenBank under the accession numbers AF079111, AF079112, AF079113, AF079114 and AF079115, respectively. Control experiments included RT-PCR reactions performed with total RNA extracted from blood since small amounts of blood contaminate stria vascularis. None of these reactions revealed appropriate products (*data not shown*). Further, RNA samples were tested to be free of DNA contamination by showing that no PCR products resulted from reactions in which RNA was not transcribed into cDNA receptor (Fig. 6, lanes marked '−').

## Discussion

The most salient findings of the present study are: a) muscarinic acetylcholine receptors are located in the basolateral membrane of SMC, b) they cause a transient

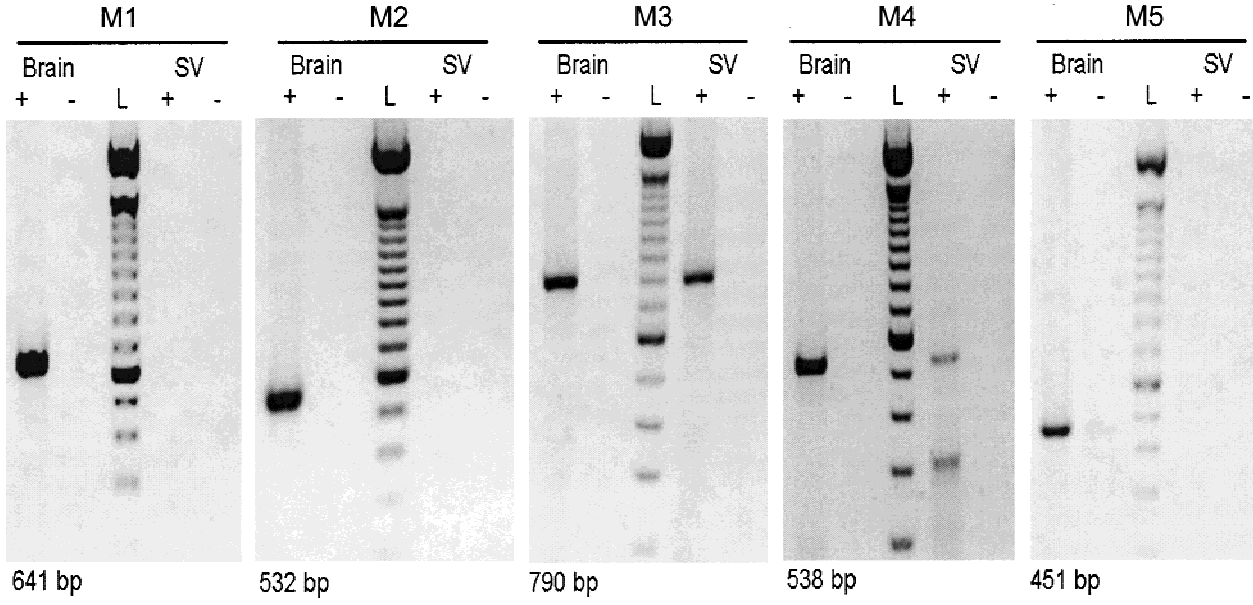


**Fig. 6.** Agarose gel electrophoresis of reverse-transcriptase polymerase chain reaction (RT-PCR) products. RT-PCR was performed with gene-specific primers for muscarinic acetylcholine receptor subtypes on 0.2–0.3 μg of total RNA obtained from microdissected stria vascularis (SV) or brain in the presence (+) and absence (−) of reverse-transcriptase. The DNA markers (L) consisted of 15 blunt-ended fragments between 100 and 1500 bp in multiples of 100 bp. Note that in SV bands of the expected sizes were found only for M3 and M4 but not for M1, M2 or M5. Further, note that in brain bands of the expected sizes were found for all subtypes. RT-PCR products were cloned and sequenced for identification. Sequences for the M1, M2, M3, M4 and M5 muscarinic acetylcholine receptor fragments are available under the accession numbers AF079111, AF079112, AF079113, AF079114 and AF079115, respectively.

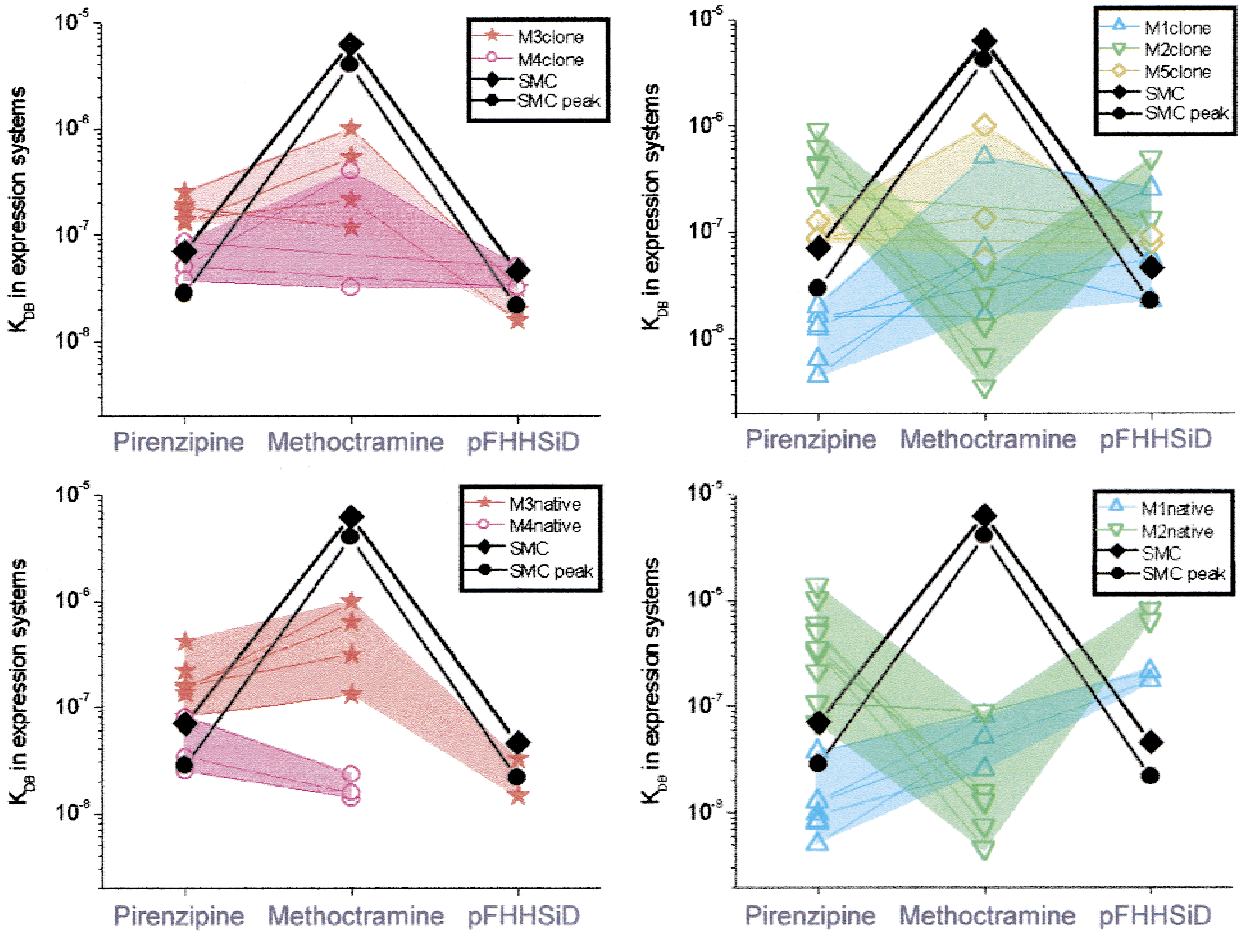


**Fig. 7.** Comparison of $K_{DB}$ values of pirenzipine, methoctramine and pFHHSiD for cloned and native muscarinic acetylcholine receptors. $K_{DB}$ values for cloned and native muscarinic acetylcholine receptors are given (*open symbols*) and high-lighted by different colors (for citations *see* Tables 2 and 3). $K_{DB}$ values obtained in the present study for the carbachol-induced transient increase in $I_{sc}$ (*filled circles*) and the carbachol-induced sustained decease in $I_{sc}$ (*filled diamonds*) are shown as well. Note that the M1, M2 and M3 muscarinic acetylcholine receptor subtypes are characterized by a distinct pattern and that the pattern found in the present study matches best the M3 subtypes.

increase and a sustained decrease of the rate of $K^+$ secretion, c) they increase $[Ca^{2+}]_i$ and therefore may include the M1, M3 and/or M5 subtype, d) muscarinic receptors in stria vascularis decrease cAMP production and therefore may include the M2 and/or M4 subtype, e) they are pharmacologically most similar to the M3 and M4 receptor subtypes and f) stria vascularis contains transcripts for the M3 and M4 muscarinic acetylcholine receptor subtypes.

## Evidence for M3 Muscarinic Acetylcholine Receptors

The findings that stria vascularis does not contain transcripts for the M1, M2 and M5 muscarinic acetylcholine receptor subtypes makes it highly unlikely that any of these receptor subtypes contributed to the functional responses observed. This conclusion is unambiguously supported by the pharmacological data with respect to the M2 receptor subtype. Indeed, $K_{DB}$ values of pirenzipine, methoctramine and pFHHSiD for clones and native receptors follow a distinctly different pattern than found in SMC (Fig. 7). Less conclusive are the pharmacological data with respect to the M1 and M5 receptor subtypes.

The finding that stria vascularis contains transcripts for the M3 and M4 muscarinic acetylcholine receptor subtypes makes it likely that one or both of these receptor subtypes contribute to the functional responses observed. Comparison of $K_{DB}$ values obtained in SMC with values obtained in cloned and native M3 and M4 receptor subtypes suggests, although not unambiguously, that M3 and M4 muscarinic acetylcholine receptors are mediating the inhibitory response on $K^+$ secretion (Fig. 7). This conclusion is supported by the finding that CCh

caused an increase in $[Ca^{2+}]_i$ that occurred with a similar time course and $EC_{50}$ than the increase in $I_{sc}$ (Fig. 2). An increase in $[Ca^{2+}]_i$ is consistent with the activation of the $G_q$/PLC/$IP_3$ signaling pathway that is typically linked to the M3-receptor subtype (Alexander et al., 1998). In addition, the observation that CCh caused a decrease in cAMP production (Fig. 3) would be consistent with activation of the $G_i$/AC signaling pathway that is typically linked to the M4-receptor subtype (Alexander et al., 1998). Consistent with this signaling pathway is the finding that stria vascularis contains adenylyl cyclase isoform 2, which is inhibited by $G_i$ (Kumagami et al., 1999; Drescher et al., 2000). Alternatively, it is conceivable that activation of the M3 receptors mediates the observed decrease in cAMP production via an inhibition of an adenylyl cyclase (Jordan, Landan & Iyengar, 2000).

### Physiological Relevance of Muscarinic Receptors in Stria Vascularis

The question regarding the physiological relevance of the muscarinic acetylcholine receptors in stria vascularis is linked to the question of whether or not these receptors are reached by agonist. Interestingly, acetylcholine is the main efferent neurotransmitter, which exerts an inhibitory effect on the sensory cells and their innervation to protect them from overstimulation (Guinan, 1996). Although stria vascularis is thought to not receive any direct innervation, it is conceivable that efferent neurotransmitters may reach SMC via the blood stream to exert an inhibitory potentially protective effect as well. This concept, however, is as of now highly hypothetical.

The support by Research Grant R01-DC-01098 from the National Institute on Deafness and Other Communication Disorders, National Institutes of Health is gratefully acknowledged.

## References

Alexander, S.P.H., Peters, J.A., Mead, A., 1998. 1998 receptor and ion channel nomenclature. Elsevier, Cambridge.

Bognar, I.T., Altes, U., Beinhauer, C., Kessler, I., Fuder, H. 1992. A muscarinic receptor different from the M1, M2, M3 and M4 subtypes mediates the contraction of the rabbit iris sphincter. *Naunyn Schmiedebergs Arch. Pharmacol.* **345:**611–618

Brauner-Osborne, H., Brann, M.R. 1996. Pharmacology of muscarinic acetylcholine receptor subtypes (m1–m5): high throughput assays in mammalian cells. *Eur. J. Pharmacol.* **295:**93–102

Buckley, N.J., Bonner, T.I., Buckley, C.M., Brann, M.R. 1989. Antagonist binding properties of five cloned muscarinic receptors expressed in CHO-K1 cells. *Mol. Pharmacol.* **35:**469–476

Caulfield, M.P., Birdsall, N.J. 1998. International Union of Pharmacology. XVII. Classification of muscarinic acetylcholine receptors. *Pharmacol. Rev.* **50:**279–290

Chen, K., Waller, H.J., Godfrey, D.A. 1995. Muscarinic receptor subtypes in rat dorsal cochlear nucleus. *Hear. Res.* **89:**137–145

Cuq, P., Magous, R., Bali, J.P. 1994. Pharmacological coupling and functional role for the muscarinic receptor subtypes in isolated cells from the circular smooth muscle of the rabbit cecum. *J. Pharmacol. Exp. Ther.* **271:**149–155

Dehaye, J.P., Marino, A., Soukias, Y., Poloczek, P., Winand, J., Christophe, J. 1988. Functional characterization of muscarinic receptors in rat parotid acini. *Eur. J. Pharmacol.* **151:**427–434

Doods, H.N., Mathy, M.J., Davidesko, D., van Charldorp, K.J., de Jonge, A., van Zwieten, P.A. 1987. Selectivity of muscarinic antagonists in radioligand and in vivo experiments for the putative M1, M2 and M3 receptors. *J. Pharmacol. Exp. Ther.* **242:**257–262

Dorje, F., Wess, J., Lambrecht, G., Tacke, R., Mutschler, E., Brann, M.R. 1991. Antagonist binding profiles of five cloned human muscarinic receptor subtypes. *J. Pharmacol. Exp. Ther.* **256:**727–733

Drescher, M.J., Khan, K.M., Hatfield, J.S., Shakir, A.H., Drescher, D.G. 2000. Immunohistochemical localization of adenylyl cyclase isoforms in the lateral wall of the rat cochlea. *Brain Res. Mol. Brain Res.* **76:**289–298

Eltze, M.1996. Functional evidence for an $alpha_{1B}$-adrenoceptor mediating contraction of the mouse spleen. *Eur. J. Pharmacol.* **311:**187–198

Goodwin, B.P., Anderson, G.F., Barraco, R.A. 1995. Characterization of muscarinic receptors in the rat nucleus tractus solitarius. *Neurosci. Lett.* **191:**131–135

Guinan, J.J., 1996. Physiology of olivocochlear efferents. *In:* The Cochlea. P. Dallos, A.N. Popper, R. Fay editors. pp. 435–502. Springer Verlag, New York.

Hulme, E.C., Birdsall, N.J., Buckley, N.J. 1990. Muscarinic receptor subtypes. *Annu. Rev. Pharmacol. Toxicol.* **30:**633–673

Jordan, J.D., Landau, E.M., Iyengar, R. 2000. Signaling networks: the origins of cellular multitasking. *Cell* **103:**193–200

Kashihara, K., Varga, E.V., Waite, S.L., Roeske, W.R., Yamamura, H.I. 1992. Cloning of the rat M3, M4 and M5 muscarinic acetylcholine receptor genes by the polymerase chain reaction (PCR) and the pharmacological characterization of the expressed genes. *Life Sci.* **51:**955–971

Kumagami, H., Beitz, E., Wild, K., Zenner, H.P., Ruppersberg, J.P., Schultz, J.E. 1999. Expression pattern of adenylyl cyclase isoforms in the inner ear of the rat by RT-PCR and immunochemical localization of calcineurin in the organ of Corti. *Hear. Res.* **132:**69–75

Lazareno, S., Birdsall, N.J. 1993. Pharmacological characterization of acetylcholine-stimulated [$^{35}$S]-GTP $\gamma$S binding mediated by human muscarinic m1–m4 receptors: antagonist studies. *Br. J. Pharmacol.* **109:**1120–1127

Lazareno, S., Buckley, N.J., Roberts, F.F. 1990. Characterization of muscarinic M4 binding sites in rabbit lung, chicken heart, and NG108-15 cells. *Mol. Pharmacol.* **38:**805–815

Liu, J., Wangemann, P. 1998. Pharmacological evidence for the M3 muscarinic receptor mediating inhibition of $K^+$ secretion in vestibular dark cells and strial marginal cells. *Assoc. Res. Otolaryngol.* **21:**113

Morley, B.J., Li, H.S., Hiel, H., Drescher, D.G., Elgoyhen, A.B. 1998. Identification of the subunits of the nicotinic cholinergic receptors in the rat cochlea using RT-PCR and in situ hybridization. *Brain Res. Mol. Brain Res.* **53:**78–87

Scherer, E.Q., Wonneberger, K., Wangemann, P. 2001. Differential desensitization of $Ca^{2+}$ mobilization and vasoconstriction by $ET_A$ receptors in the gerbil spiral modiolar artery. *J. Membrane Biol.* **182:**183–191

Shimozono, M., Scofield, M.A., Wangemann, P. 1998. Molecular evidence for muscarinic receptor subtypes in stria vascularis and vestibular labyrinth. *Assoc. Res. Otolaryngol.* **21:**113

Waelbroeck, M., Tastenoy, M., Camus, J., Christophe, J. 1990. Binding of selective antagonists to four muscarinic receptors (M1 to M4) in rat forebrain. *Mol. Pharmacol.* **38:**267–273

Wangemann, P.1995. Comparison of ion transport mechanisms be-

tween vestibular dark cells and strial marginal cells. *Hear. Res.* **90:**149–157

Wangemann, P., Liu, J., Marcus, D.C. 1995. Ion transport mechanisms responsible for $K^+$ secretion and the transepithelial voltage across marginal cells of stria vascularis in vitro. *Hear. Res.* **84:**19–29

Wangemann, P., Liu, J., Shiga, N. 1996. Vestibular dark cells contain the $Na^+/H^+$ exchanger NHE-1 in the basolateral membrane. *Hear. Res.* **94:**94–108

Wangemann, P., Liu, J., Shimozono, M., Schimanski, S., Scofield, M.A. 2000. $K^+$ secretion in strial marginal cells is stimulated via $\beta_1$-adrenergic receptors but not via $\beta_2$-adrenergic or vasopressin receptors. *J. Membr. Biol.* **175:**191–202

Wangemann, P., Liu, J., Shimozono, M., Scofield, M.A. 1999. $\beta_1$-adrenergic receptors but not $\beta_2$-adrenergic or vasopressin receptors regulate $K^+$ secretion in vestibular dark cells of the inner ear. *J. Membrane Biol.* **170:**67–77